

Does $(\text{TaSe}_4)_2\text{I}$ really harbor an axionic charge density wave?


Cite as: Appl. Phys. Lett. **120**, 063102 (2022); <https://doi.org/10.1063/5.0080380>

Submitted: 30 November 2021 • Accepted: 03 January 2022 • Published Online: 08 February 2022

 A. A. Sinchenko, R. Ballou,  J. E. Lorenzo, et al.

COLLECTIONS

Paper published as part of the special topic on [One-Dimensional van der Waals Materials](#)

 This paper was selected as Featured



View Online



Export Citation



CrossMark

ARTICLES YOU MAY BE INTERESTED IN

[Excess noise in high-current diamond diodes](#)

Applied Physics Letters **120**, 062103 (2022); <https://doi.org/10.1063/5.0083383>

[Automatic electron hologram acquisition of catalyst nanoparticles using particle detection with image processing and machine learning](#)

Applied Physics Letters **120**, 064103 (2022); <https://doi.org/10.1063/5.0074231>

[Optical interface for a hybrid magnon–photon resonator](#)

Applied Physics Letters **120**, 062404 (2022); <https://doi.org/10.1063/5.0075908>

 QBLOX



1 qubit

Shorten Setup Time

Auto-Calibration
More Qubits

Fully-integrated

Quantum Control Stacks
Ultrastable DC to 18.5 GHz
Synchronized <<1 ns
Ultralow noise



100s qubits

[visit our website >](#)

Does $(\text{TaSe}_4)_2\text{I}$ really harbor an axionic charge density wave?

Cite as: Appl. Phys. Lett. **120**, 063102 (2022); doi: [10.1063/5.0080380](https://doi.org/10.1063/5.0080380)

Submitted: 30 November 2021 · Accepted: 3 January 2022 ·

Published Online: 8 February 2022





View Online



Export Citation



CrossMark

A. A. Sinchenko,^{1,2,a)}  R. Ballou,^{3,4} J. E. Lorenzo,^{3,4}  Th. Grenet,^{3,4}  and P. Monceau^{3,4,a)}

AFFILIATIONS

¹M.V. Lomonosov Moscow State University, 119991 Moscow, Russia

²Kotelnikov Institute of Radioengineering and Electronics of RAS, 125009 Moscow, Russia

³University Grenoble Alpes, Institute Neel, F-38042 Grenoble, France

⁴CNRS, Institute Neel, F-38042 Grenoble, France

Note: This paper is part of the APL Special Collection on One-Dimensional van der Waals Materials.

a) Authors to whom correspondence should be addressed: aasinch@mail.ru and pierre.monceau@neel.cnrs.fr

ABSTRACT

A recent experimental work has reported an excess of the non-linear conductivity in the charge density wave (CDW) sliding mode of the quasi one-dimensional compound $(\text{TaSe}_4)_2\text{I}$, when a magnetic field is applied co-linearly to the electric field [Gooth *et al.*, Nature **575**, 315 (2019)]. This result has opened a conceptual approach, where the CDW gap in $(\text{TaSe}_4)_2\text{I}$ is opened between Weyl fermions of opposite chirality with the assumption that this compound is a Weyl semi-metal in its undistorted high temperature phase. We report measurements in the sliding state of $(\text{TaSe}_4)_2\text{I}$ performed in similar conditions. We have found no increase in the magnetoconductivity. In our attempts for understanding this unsettling discrepancy, we stress the specific nature of the Peierls transition in $(\text{TaSe}_4)_2\text{I}$ and the strong electron-phonon coupling present in this compound. Given the lack of further evidence, we think that it is premature to assert that $(\text{TaSe}_4)_2\text{I}$ is an axionic insulator.

Published under an exclusive license by AIP Publishing. <https://doi.org/10.1063/5.0080380>

Experimental and theoretical investigations in condensed matter can allow for the realization of quantum field theory predictions such as the axion electrodynamics.¹ The axion particle has become a candidate responsible for some or all of the dark matter of the universe.² The search for experiment detection of an axion has been recently reviewed,³ and an experiment proposal is under way.⁴

Since the discovery of three-dimensional (3D) topological insulators,⁵ much interest has been devoted to Weyl semi-metals (see Ref. 6 for a recent review). They are materials in which low energy electronic quasi-particles behave as chiral relativistic fermions without rest mass known as Weyl fermions. Weyl fermions exist at isolated crossing points between conduction and valence bands, called Weyl nodes. Axion electrodynamics in Weyl semi-metals arise from the separation of Weyl nodes of opposite chirality in momentum space and energy. Turning on interactions, chiral symmetry breaking is the phenomenon of the spontaneous generation of an effective mass of Weyl fermions, namely, a pairing between the fermions (electrons) and holes with different chiralities, which opens gaps at the Weyl points and induces a charge density wave (CDW). The opening of this gap transforms the Weyl semi-metal into an axion insulator, and the phase of the CDW is

identified to the dynamic axion field θ .⁷ The CDW phason is the axion mode, and its dynamics is, therefore, described by the topological term $\theta E \cdot B$. The CDW phason mode is also known as the Goldstone mode. Applying B collinearly to E leads to an extra chiral flow of charges, which can be detected from magnetoelectric measurements.

Recently, a gigantic negative longitudinal magnetoresistance (LMR) was observed⁸ in the CDW compound $(\text{TaSe}_4)_2\text{I}$ when the magnetic field co-linear to the electric field is applied parallel to the CDW direction. Such a LMR appears only in the state of collective CDW motion (sliding) at electric fields larger than the characteristic threshold electric field, E_r . The authors concluded that the LMR results from a chiral anomaly appearing in the Peierls state of $(\text{TaSe}_4)_2\text{I}$ and originating from the anomalous axionic contribution to the phason current. This result was considered as the first determination of the occurrence of axion electrodynamics in condensed matter,^{7,9} reinforcing the concept of an axionic charge density wave.¹⁰

Oddly, and in contrast to the results reported in Ref. 8, the LMR measured by Cohn *et al.*¹¹ was positive and did not exceed a fraction of per cent in the sliding as well as in the static regimes of the CDW in the temperature range down to 30 K. The main difference between

both experiments is the sample geometry and the position of the contacts: in Ref. 8, massive single crystals with a cross section of order $10^3\text{--}10^4 \mu\text{m}^2$ and the length between the potential contacts 3–10 mm were used, whereas in Ref. 11, very thin samples in the order $10 \mu\text{m}^2$ of the cross section and distances between the edges of the contacts of order $10^2 \mu\text{m}$ were used.

In view of this strong disagreement, we have repeated the measurements of the non-linear state of $(\text{TaSe}_4)_2\text{I}$ under a magnetic field. To that end, we have set experimental conditions mostly identical to those in Ref. 8 using nearly the same sample geometry, the same contact preparation method, and the same measurement setup. We have not found any significant contribution of the magnetic field in the sliding motion of the CDW. We discuss the possible reasons of the discrepancy including the generation of CDW dislocations under a strong thermal gradient, and we stress the role of the strong electron-phonon coupling in $(\text{TaSe}_4)_2\text{I}$.

$(\text{TaSe}_4)_2\text{I}$ is a chain-like material displaying a Peierls phase transition (for a review on the Peierls transition and compounds, see Refs. 12 and 13) at $T_P \approx 263 \text{ K}$, and this value varies rather strongly that has been intensively studied since several decades.^{14,15} $(\text{TaSe}_4)_2\text{I}$ crystallizes with tetragonal symmetry (space group I422) and consists of TaSe_4 van der Waals chains parallel to the c -axis separated by iodine atoms. In an TaSe_4 infinite chain, each Ta is sandwiched by two nearly rectangular selenium units forming a Se_2^{-2} pair. The dihedral angle between adjacent rectangles is almost 45° (44° and 46°), so the Ta atom is located at the center of a rectangular anti-prism of eight Se atoms.¹⁴ The interaction between Ta atoms is through d_{z^2} overlap along the chain. (The shortest interchain metal-metal distance is about 6.7 \AA to be compared to the intrachain average value d of about 3.2 \AA .)

Band structure calculations¹⁶ suggest a single d_{z^2} electronic band at the Fermi level. This band is $1/4$ filled with one free electron per $\text{Ta}^{+4} \text{Ta}^{+5} 4\text{Se}^{-2} 2\text{I}^-$ formula unit. Consecutive Ta atoms occupy two alternating nonequivalent sites, but the Ta-Ta distance is unique, $d_{\text{Ta-Ta}} = 3.206 \text{ \AA}$. Owing to the Se_4 -unit rotation pattern, the crystallographic unit cell parameter is $c = 4d_{\text{Ta-Ta}}$. On that basis, one may expect $(\text{TaSe}_4)_2\text{I}$ to be an insulator, because the Fermi wave vector corresponds to a Brillouin zone boundary: $k_F = 1/4(\pi/d_{\text{Ta-Ta}}) = \pi/c = c^*/2$. Assuming that Coulomb repulsion favors an antiphase arrangement of CDWs on adjacent chains, one expects the CDW satellites below T_P to appear at or near c^* and $-a^*$ or c^* and $-b^*$ close to the allowed Bragg reflections, G , of the parent undistorted structure. Indeed electron and x-ray diffraction experiments¹⁷ below T_P show the appearance of eight first-order satellites around each room-temperature reflection at incommensurate positions of the type $G + (\pm\delta h, \pm\delta k, \pm\delta l)$ close to each main Bragg reflection $G = (H, K, L)$ with $\delta h = \delta k = 0.045$ and $\delta l = 0.085$, effectively very near of the Brillouin zone center. These eight satellites correspond to four degenerate domains with single incommensurate modulation, single q -domains with orthorhombic or identically stable monoclinic symmetry.¹⁸

The atomic displacements of the modulated CDW state consist of two parts: the major one^{17,19} is a transverse acoustic-like wave (perpendicular to q) with equal amplitudes of all atoms (0.13 \AA) and a periodicity involving mostly z -polarized Ta displacements that corresponds to a LLSS pattern of long and short in-chain Ta-Ta distances (Ta-tetramerization modes), which represents the CDW. The amplitude of the displacements of this tetramerization is one order of

magnitude smaller than that of the acoustic component and is only detectable by using x-ray anomalous scattering techniques.²⁰ Since the electronic variables are unlikely to couple directly to such a long-wavelength acoustic shear wave, a model has been proposed,¹⁹ in which the soft Ta-tetramerization modes interact with the acoustic degrees of freedom and induce the condensation of a mixed acoustic/optic ionic modulation. In this model, the values of the satellite wave vector components are not related to the topology of the Fermi surface (FS). They are determined by the strength of the gradient interaction terms between optical and acoustic degrees of freedom. Similar to models developed in the context of incommensurate long-wavelength modulated dielectrics such as quartz, the incommensurate structure arises from the presence of a pseudo-Lifshitz invariant involving an optical order parameter and the elastic deformations.¹⁹ The presence and further detection of the Ta-tetramerization²⁰ provides the key for understanding the mechanism of the phase transition at T_P , which can be described as a Brillouin zone center Peierls instability.

The FS of $(\text{TaSe}_4)_2\text{I}$ has been mapped by angle-resolved photoelectron spectroscopy (ARPES).²¹ It consists of parallel planes oriented perpendicularly to the chain direction. The dispersion of the d_{z^2} band has also been recorded²² at $T = 300 \text{ K}$ for a range of wavevectors along the 1D chain direction. The band shows a strong dispersion throughout the first Brillouin zone with minimum at Γ , the center of the Brillouin zone, also detectable with weaker intensity in the second and third Brillouin zones. The low intensity at E_F for wave vectors close to k_F is the indication of a pseudogap still presents above the Peierls transition temperature. The temperature dependence of the optical conductivity exhibits a strong absorption due to the CDW gap. This gap is already present in the electronic excitation spectrum above the Peierls transition manifesting that, even at high temperature free carriers, are condensed into a fluctuating CDW ground state. However, above T_P , as shown by neutron¹⁹ or x-rays scattering,¹⁷ the CDW does not exhibit long-range order but has the physical properties of a liquid. Below T_P , this “liquid” condensate crystallizes into a superlattice structure. Optical spectra show a nearly continuous change between 15 and 300 K. The shape of the longitudinal optical conductivity spectrum exhibits just a continuous narrowing through the Peierls transition. Recent ARPES measurements are also in agreement with the gapless nature of $(\text{TaSe}_4)_2\text{I}$ at room temperature and reveal its characteristic dispersion.²³

Single crystals of $(\text{TaSe}_4)_2\text{I}$ were grown by direct combination of the elements in sealed quartz tubes in a gradient furnace at a temperature ranging from 850°C to 900°C with iodine as a transport agent.¹⁵ For the experiments, we selected single crystals with nearly the same size as those studied in Ref. 8. Contacts for electrical transport measurements in the four-probe configuration have been prepared using thin gold wires glued on the sample by silver paste. All current-voltage characteristics (IVc) and resistance measurements were carried out in the current mode. To exclude possible heating effects, a part of the sample was covered by highly heat-conducting epoxy as it was done in Ref. 8, and another part of the sample was covered by apiezon grease as we usually do it for such experiments. Magnetotransport measurements were performed at two mutually perpendicular orientations of the magnetic field in the field range up to 8 T using a superconducting solenoid.

The temperature dependence of the three studied samples displayed the same behavior: a strong monotonic growth of the resistance

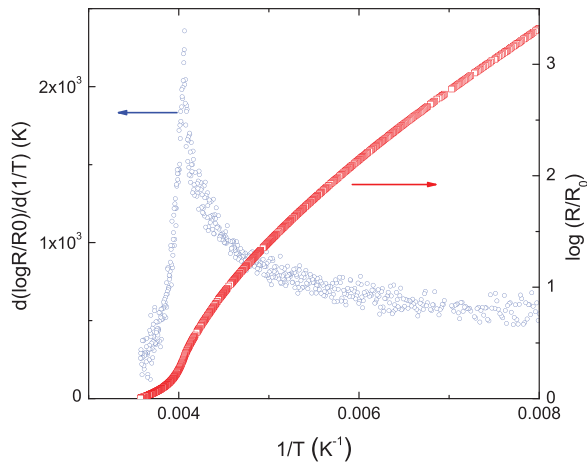


FIG. 1. Logarithm of the electrical resistance, R , normalized to the $R_0 = R(300\text{ K})$ (right axis, red) and its logarithmic derivative (left axis, blue) as a function of the inverse temperature.

with a decrease in temperature (Fig. 1, right axis). A pronounced peak is observed in the logarithmic derivative, $d[\log(R/R_0)]/d(1/T)$ vs the inverse temperature (Fig. 1, left axis). The position of this peak determines the transition into the CDW state;^{24,25} the value of which is $T_P = 248\text{ K}$ in our samples. It has been often argued that differences in T_P values reflect small deviations from stoichiometry (loss of iodine). In that case, one expects the change in the value of T_P to be correlated with a change in the conduction electron Fermi wavevector and, consequently, in the satellite position. No such correlation was observed.¹⁹ We shall come back to this point below.

Measurements of IVc on the samples covered by epoxy demonstrated a strong monotonic decrease in the resistance with an increase in the current without exhibiting a strong threshold behavior at the onset of the CDW sliding regime, probably due to Joule heating. We only observed sharp threshold characteristics for samples covered by apiezon. Figure 2(a) shows a set of such characteristics for one of the

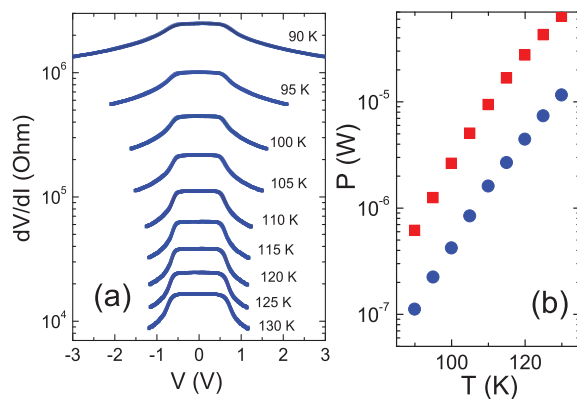


FIG. 2. (a) Differential current-voltage characteristics, $dV/dI(V)$, in one of the samples demonstrating the CDW collective motion in the temperature range 90–130 K. (b) Joule power dissipated at the threshold electric field, $P(E_t)$ (blue circles) and at twice the threshold, $P(2E_t)$ (red squares) as a function of temperature.

samples in the temperature range 90–130 K. In Fig. 2(b), we show the temperature dependence of the Joule power, P , dissipated at the threshold voltage (blue circles) and at twice the threshold voltage (red squares). It can be seen that Joule power increases as the temperature increases, qualitatively in the same way as it was reported in Ref. 8 but with a difference of nearly three orders of magnitude.

The main experimental result of the present work is obtained from measurements under magnetic field, B . Figure 3(a) shows differential IVc at $T = 90\text{ K}$ at $B = 0\text{ T}$ (green), at $B = 7\text{ T}$ (red) with the magnetic field aligned parallel to the c -axis (chain direction) and collinear with the electric field, E , and in the transverse orientation (blue) with B and E perpendicular. It can be seen that the effect of the magnetic field is negligibly small as it was also found in Ref. 11. Moreover, the magnetoresistance is positive both for transverse and longitudinal orientation of B . As an example, Fig. 3(b) shows the result of the direct measurement of the magnetoresistance, $MR = \frac{R(B) - R(0)}{R(0)}$, swiping B from 0 to 7 T in the case of B parallel to I with the applied current of $I = 6 \times 10^{-4}\text{ mA}$ just corresponding to the sliding state of the CDW. It can be seen that the MR is positive, very small (of order 10^{-3}) and follows a quadratic dependence on the magnetic field.

Gooth *et al.*⁸ have measured a longitudinal MR in the sliding state of $(\text{TaSe}_4)_2\text{I}$, which has been considered as the first experimental observation of the axion dynamics in condensed matter. Our results, as well as those of Ref. 11, do not show any manifestation of the magnetoresistance. In the following, we discuss some points that may serve to illustrate the difficulty to reconcile the actual features of $(\text{TaSe}_4)_2\text{I}$ with the Weyl semi-metal physics and the axion electrodynamics.

$(\text{TaSe}_4)_2\text{I}$ was characterized as a semi-metal, which undergoes a phase transition by breaking of the chiral symmetry between Weyl nodes (WP). From first principles calculations, $(\text{TaSe}_4)_2\text{I}$ is described as a semi-metal²⁶ with coupled WP by e - e interactions that yield the opening of a gap and the onset of a CDW. It is found that the entire Fermi surface is formed from topological bands connecting bulk chiral fermions. In the electronic structure, 48 WPs within 15 meV of E_F are found.

The same authors performed x-ray diffraction experiments in their samples.²⁶ A set of eight satellites, appearing at positions

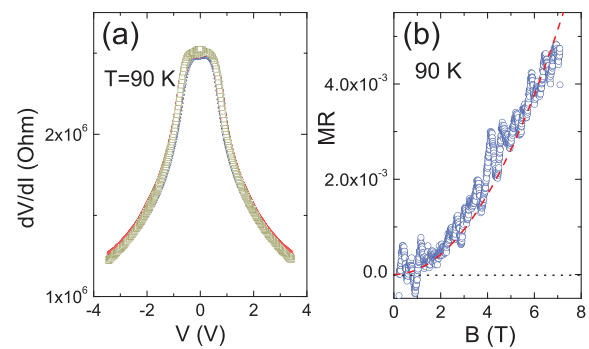


FIG. 3. (a) Differential current-voltage characteristics, $dV/dI(V)$, at $T = 90\text{ K}$ in magnetic field $B = 0\text{ T}$ (dark yellow symbols), magnetic field $B = 7\text{ T}$ parallel to the current (red symbols) and $B = 7\text{ T}$ perpendicular to the current (blue symbols). (b) Magnetoresistance of the same $(\text{TaSe}_4)_2\text{I}$ sample at $T = 90\text{ K}$ in a magnetic field parallel to the current $I = 1.2I_t$, where I_t is the threshold current for the CDW sliding.

$(\pm\eta, \pm\eta, \pm\delta)$, are obtained at $\eta = 0.027$, and $\delta = 0.012$ and $T_p = 248$ K. However, this CDW modulation wavevector is much shorter than the nesting vectors between WPs. These nesting vectors can be approximated to the closest integer number of the experimental CDW wave vector h, h, k such as $q_{WP} = mh, nk, ol$ with values of m, n , and o ranging from 0 to 20 that yield the authors²⁶ “to suggest that FWs’ nesting is not itself the origin of the CDW.” Thus, the suggested electronic CDW does not nest the Weyl points and, therefore, does not break the chiral symmetry. The broken symmetry originates from e–ph coupling between pieces of the Fermi surface separated by the q vector. To end this paragraph on the components of the CDW modulation wavevector, these values contrast with those reported in Refs. 17, 19, and 20: $\eta = 0.045 \pm 0.005$ and $\delta = 0.085 \pm 0.005$ in the nominally pure compound. A smaller value agrees with the results in Nb-doped samples.¹⁹

More importantly, the authors describe $(\text{TaSe}_4)_2\text{I}$ as an assembly of nearly independent infinite (TaSe_4) chains with a very weak interchain coupling. That is not corroborated by elastic neutron scattering,¹⁹ which shows that above T_p the inverse correlation lengths along the three directions c^* , $a^* + b^*$, and $a^* - b^*$ are nearly isotropic with an anisotropy parameter amounting to 1.8. 40 K above T_p , the average number of correlated chains was estimated at around 200. The strong interchain interactions of the CDW, which are at variance with those typically found for other quasi-1D conductors, are also manifested in the long wavelength acoustic character of the atomic displacements, as has been explained above. This strong interaction with the underlying lattice was lacking in this work,²⁶ as well.

The possibility that the CDW can slide was suggested by Fröhlich²⁷ and studied by Allender *et al.*²⁸ in a tight binding model. If the lattice wave moves with the electrons with velocity v_s , the CDW order parameter will vary as: $\Delta = |\Delta| \exp(2ik_F(x - v_s t))$. In a 1D model, the two planes of the FS are at $(-\pi/k_F) + q$ and $(+\pi/k_F) + q$ with $m^* v_s = \hbar q$, where m^* is the effective electronic mass, which yield, in the static reference frame, a current $J = nev_s$, where n is the number of electrons in the band affected by the CDW. The CDW velocity can be measured from the periodic signal superposed to be the static non-linear current, the so-called narrow band noise (NBN) or from the Shapiro steps structure when the motion of the CDW is locked by an applied external rf field. Thus, the energy gap reduces the elastic scattering of individual electrons, because there is no state for energy relaxation. The properties of this nonlinear state have been studied in detail for quasi-1D materials with different crystallographic symmetries, where chirality does not play any role. Note that the $\hbar k_F$ term makes the difference in energies between the left- and right-band sides of the displaced distribution.

In the case in which the ground CDW state is an axion insulator, in addition to the Fröhlich Hamiltonian, a supplementary axion term (similarly to the quantum field theory) was added^{8,29} containing the contribution $\theta E \cdot B$ of the chiral anomaly in the undistorted Weyl semi-metal, with θ being the dynamical axion field identified to the dynamics of the phase of the CDW. There is, thus, an extra contribution to the phason current from this chiral anomaly and an excess conductivity in the sliding state. In addition to the electric force which, above the depinning electric field from impurities, makes the CDW to slide, there is an extra force that increases the CDW velocity and, therefore, the nonlinear current. This effect is similar to the case where the velocity of a CDW in the sliding state is increased by the

application of an independent current on a small part of the sample.³⁰ This result also illustrates the very long range coherence of the CDW motion.

Let us now consider the experimental results of Ref. 8. The non-linearity in the IV characteristics has been essentially studied in one crystal (A). The data do not exhibit a real sharp threshold for the onset of the CDW sliding but rather a continuous decrease in the resistance. More surprisingly, this non-linearity in the IV characteristics is only seen at $T < 180$ K much below the Peierls transition temperature, when previous results show that the sliding occurs immediately below T_p with temperature dependent E_t . When a magnetic field is applied collinearly with the electric field, a sharper decrease in the resistivity in the non-linear state is observed at very delimited conditions: at a single temperature, namely, $T = 80$ K and under a very large applied voltage. This effect is quantified by measuring the magnetoconductivity as: $\Delta(dI/dV)_B = (dI/dV)_B - (dI/dV)_{0T}$. The most disturbing result is the temperature dependence of $\Delta(dI/dV)_B$ in Fig. 3(h) of Ref. 8. It is null down to 120 K, and it sharply increases at 80 K. The data for samples A and B at $T = 105$ K, with B and E collinear shown in the extended data Figs. 8(a) and 8(b) for sample A and 8(d) and 8(e) for sample B, are very similar to our results shown in Fig. 3. Something else occurs between 105 and 80 K, which is not explained in Ref. 8.

In our work (see Fig. 2), as well as in previously published studies^{24,25,31} in $(\text{TaSe}_4)_2\text{I}$, the relative resistance drop $R(E < E_t)/R(4E_t)$ at $T = 80 - 120$ K is small not more than a factor of 2. In contrast, in Ref. 8, this relation is more than ten times larger at zero magnetic field and near 100 times larger at $B = 9$ T. The gigantic heating effect in Ref. 8, which takes place at high bias ought to be considered. Indeed, the authors have estimated Joule heating only at the threshold voltage determined as $V_t = 6$ V at 80 K and obtained for $P \approx 20 \mu\text{W}$ that is really small enough. However, at $V = 27$ V (near $4E_t$), this power is already $P \approx 60$ mW that is more than three order of magnitude larger. However, at 105 K, these values are in the range of 200 mW. In comparison, the power dissipated in our work at $T = 90$ K is $P = 0.1 \mu\text{W}$ at the threshold and $\approx 3 \mu\text{W}$ at four times the threshold. This is two order of magnitude smaller than in Ref. 8 at the same condition and $T = 80$ K. As a result, one may consider that the main contribution to the resistance drop in Ref. 8 may originate as a consequence of heating (as we discuss below), while the contribution of the CDW sliding to the total drop of resistance may be less than 10%. This is simply one order of magnitude smaller than the magnetoresistance effect and reported as an indication of axion transport in $(\text{TaSe}_4)_2\text{I}$.

Transport properties in quasi 1D metals have been studied under the assumption that the single particle gap originates from the nesting of a single band at $+k_F$ and $-k_F$. This mechanism, the Peierls instability, stands for the large part of the CDW compounds. However a large difference occurs when the CDW order opens a gap between Weyl fermions of opposite chirality. Unlike the single-band CDW ground state, the involvement of multibands in Weyl-CDW compounds results in a gapless CDW collective mode that does not contribute to the conductivity unless the Weyl cones are tilted.³² Considering the simplest two-band Weyl model in the undistorted phase, it consists of two small Fermi pockets around each Weyl node, separated by the wave vector q (that determined by x-ray scattering to be consistent with previous results). At the CDW phase transition, there is condensation of particle-hole pairs consisting of a hole in one Fermi pocket and an electron separated by momentum q . These electron and hole states

exhibit the same velocity, unlike for a 1D CDW. Thus, for the sliding mode to contribute to the DC conductivity in a Weyl-CDW, it must have an asymmetry between the velocities in different Weyl pockets. This can be accomplished by shifting the nodes in energy or inducing a tilt to the Weyl cones. Is it the case for $(\text{TaSe}_4)_2\text{I}$? We note, however, that the sliding properties of $(\text{TaSe}_4)_2\text{I}$ are very similar to those of other materials exhibiting CDW sliding.

An important point from the experimental point of view is how Joule power dissipated in the sample can lead to a strong anisotropic magnetoresistance effect. Strong heating creates strong thermal inhomogeneities, because the thermal exchange can be different at different parts of the sample. Logically, one assume that such an exchange will be better from the bottom surface of the sample, which is in contact with the high thermal conductivity substrate compared with the top surface of the sample. Such a difference leads to a strong thermal gradient from top to the bottom of the crystal, which creates a corresponding thermoelectric current. Being oriented transverse to the applied electric field, this current does not give a contribution to the total drop of voltage. There will be no effect under the application of a magnetic field parallel to this thermal current ($B \perp I$ configuration), because the Lorentz force is zero for thermo-electrons. Another picture should be observed when $B \parallel I$. In this case, the thermoelectric current, which continuously increases with the increase in the transport current, is affected by the Lorentz force that leads to an additional scattering and additional heating correspondingly.

As said before, the CDW ground state has a very long range order. However, the CDW cannot solely be assumed to behave elastically when the CDW velocity passes through strong and isolated sharp discontinuities. The conflict between different winding rates at the interface separating regions with different velocities is released by phase slippage. In a path surrounding these vortices, the phase changes by 2π . The topological defects of incommensurate CDW are dislocations very similar to vortices in superfluids, and their properties are close of those of dislocation lines in crystals. There are simple cases of dislocations: screw dislocations parallel to the chains and edge dislocations perpendicular to chains with a dislocation core with dimensions $\xi_p \xi_p$ for an edge or $\xi_p \xi_{\parallel}$ for a screw, where ξ_p and ξ_{\parallel} are the BCS amplitude coherence lengths. The CDW can be pinned at the surface, near strong impurities in the volume, at the electrodes. It was also shown that the coherence of the CDW motion is broken when a thermal gradient is applied^{33–35} between electrodes with detection of two different velocities. As the CDW order parameter is suppressed in the dislocation core, the properties of the Weyl semi-metal, which are characterized by the negative MR, could partially be restored. However, in this scenario, the amplitude of the negative MR should be very small, because this effect takes place in a relatively small part of the sample. However, if the properties of the Weyl semi-metal are to be truly restored, it should also be accompanied by a significant (at least tens of per cent) positive transverse MR that was not observed in Ref. 8.

In the context of the axion insulator, Wang and Zhang⁷ have identified the CDW dislocations as axion strings. An axion string is a one-dimensional dislocation of the axion field around which the axion field θ changes by 2π . Such chiral modes would carry a dissipationless current. It appears from Ref. 8 that the magnetoconductivity is only observed when the Joule power dissipated surpasses some threshold: 60 mW at $T = 80$ K, 200 mW at $T = 105$ K, and no effect at higher temperature. Then one may think that at this so high power dissipated, in this system

out of equilibrium, amplitude modes are excited and “hot” filaments in which the CDW order parameter is suppressed can cross at high velocity from one electrode to the other. The interaction between dislocations in the lattice and dynamical axion strings has also been studied.³⁶

In conclusion, the result of the magneto-conductivity in the sliding state of $(\text{TaSe}_4)_2\text{I}$ has raised much interest since it provides the experimental proof, which lacked, of the axion dynamics in condensed matter.⁸ This proposition originates from the chirality of the I422 space group in which it crystallizes. Here, we have raised some points, which question this statement. The 24 Weyl points derived from first principles calculations are connected with q vectors that are irrelevant with the actual CDW q -vector determined by x rays three decades ago. The distorted phase of $(\text{TaSe}_4)_2\text{I}$ consists of the condensation of a mixed acoustic/optic ionic modulation from the interaction of a T-tetramerization with a transverse acoustic wave. Thus, the symmetry breaking in $(\text{TaSe}_4)_2\text{I}$ results from electron-phonon interactions and not from electron-electron ones. The Peierls transition, probably of the first order, is rather an order-disorder transition than a displacive one. Our results do not show any extra conductivity in the sliding state of $(\text{TaSe}_4)_2\text{I}$, when magnetic and electric fields are collinear. A detailed analysis of magneto-conductivity data of Ref. 8 shows that it has only been detected abruptly below 100 K and specifically at a single temperature, $T = 80$ K (while the phase transition is at $T = 263$ K) and under a very high voltage, which induces a large Joule power dissipation. As a possible explanation of the discrepancy between our results as well as those from Ref. 11, we have suggested possible hot filaments with cores having the properties of the normal state.

We do not disregard all these fascinating theoretical and experimental discoveries around Weyl semimetals. We, however, think that, on the basis of present magneto-conductivity results, the assertion that $(\text{TaSe}_4)_2\text{I}$ would be an axionic charge density wave is not justified, and this conclusion should be considered as, at least, premature. New transport experiments are necessary for the temperature dependence of the axionic magnetoresistance in a large temperature scale and under different thermal gradients. Measurements of Shapiro steps in the sliding state will also allow us to determine if the application of a collinear magnetic field increases the CDW velocity and, therefore, if the axion field acts on the CDW long range condensate.

We are grateful to Helmut Berger for providing the samples used in this work.

AUTHOR DECLARATIONS

Conflict of Interest

We wish to confirm that there are no known conflicts of interest associated with this publication and there has been no significant financial support for this work that could have influenced its outcome.

DATA AVAILABILITY

The data that support the findings of this study are available from the corresponding authors upon reasonable request.

REFERENCES

- ¹R. D. Peccei and H. R. Quinn, *Phys. Rev. Lett.* **38**, 1440 (1977); *Phys. Rev. D* **16**, 1791 (1977); S. Weinberg, *Phys. Rev. Lett.* **40**, 223 (1978); F. Wilczek, *ibid.* **40**, 279 (1978).

- ²J. Preskill, M. B. Wise, and F. Wilczek, *Phys. Lett. B* **120**, 127 (1983); L. F. Abbott and P. Sikivie, *ibid.* **120**, 133 (1983); M. Dine and W. Fischler, *ibid.* **120**, 137 (1983).
- ³P. Sikivie, *Rev. Mod. Phys.* **93**, 015004 (2021); L. Di Luzio, M. Giannotti, E. Nardi, and L. Visinelli, *Phys. Rep.* **870**, 1 (2020).
- ⁴T. Grenet, R. Ballou, Q. Baso, K. Martineau, P. Perrier, P. Pugnat, J. Quevillon, N. Roch, and C. Smith, [arXiv:2110.14406](https://arxiv.org/abs/2110.14406) (2021).
- ⁵M. Z. Hasan and C. L. Kane, *Rev. Mod. Phys.* **82**, 3045 (2010).
- ⁶B. Q. Lv, T. Qian, and H. Ding, *Rev. Mod. Phys.* **93**, 025002 (2021).
- ⁷Z. Wang and S.-C. Zhang, *Phys. Rev. B* **87**, 161107(R) (2013).
- ⁸J. Gooth, B. Bradlyn, S. Honnali, C. Schindler, N. Kumar, J. Noky, Y. Qi, C. Shekhar, Y. Sun, Z. Wang, B. A. Bernevig, and C. Felser, *Nature* **575**, 315 (2019).
- ⁹A. Sekine and K. Nomura, *J. Appl. Phys.* **129**, 141101 (2021).
- ¹⁰D. M. Nenko, C. A. C. Garcia, J. Gooth, C. Felser, and P. Narang, *Nat. Rev. Phys.* **2**, 682 (2020).
- ¹¹I. A. Cohn, S. G. Zytsev, A. P. Orlov, and S. V. Zaitsev-Zotov, *JETP Lett.* **112**, 88 (2020).
- ¹²G. Grüner, *Density Waves in Solids* (Perseus Pub., Cambridge, MA, 2000).
- ¹³P. Monceau, *Adv. Phys.* **61**, 325 (2012).
- ¹⁴P. Gressier, A. Meerschaut, L. Guemas, J. Rouxel, and P. Monceau, *J. Solid State Chem.* **51**, 141 (1984).
- ¹⁵P. Gressier, L. Guemas, and A. Meerschaut, *Acta Cryst. B* **38**, 2877 (1982).
- ¹⁶P. Gressier, M. H. Wangbo, A. Meerschaut, and J. Rouxel, *Inorg. Chem.* **23**, 1221 (1984).
- ¹⁷K. B. Lee, D. Davidov, and A. J. Heeger, *Solid State Commun.* **54**, 673 (1985).
- ¹⁸Y. Zhang, L.-F. Lin, A. Moreo, S. Dong, and E. Dagotto, *Phys. Rev. B* **101**, 174106 (2020).
- ¹⁹J. E. Lorenzo, R. Currat, P. Monceau, B. Hennion, H. Berger, and F. Levy, *J. Phys.: Condens. Matter* **10**, 5039 (1998).
- ²⁰V. Favre-Nicolin, S. Bos, J. E. Lorenzo, J.-L. Hodeau, J.-F. Berar, P. Monceau, R. Currat, F. Levy, and H. Berger, *Phys. Rev. Lett.* **87**, 015502 (2001).
- ²¹S. Hüfner, R. Claessen, F. Reinert, T. Straub, V. N. Stocov, and P. Steiner, *J. Electron Spectrosc. Relat. Phenom.* **100**, 191 (1999).
- ²²J. Voit, L. Perfetti, F. Zwick, H. Berger, G. Margaritondo, G. Grüner, H. Höchot, and M. Grioni, *Science* **290**, 501 (2000).
- ²³X.-P. Li, K. Deng, B. Fu, Y. Li, D.-S. Ma, J. Han, J. Zhou, S. Zhou, and Y. Yao, *Phys. Rev. B* **103**, L081402 (2021).
- ²⁴M. Renard, J. Richard, M. C. Saint-Lager, and Z. Z. Wang, in *Charge Density Waves in Solids*, Lecture Notes in Physics Vol. 217, edited by Gy. Hutiray and J. Solyom (Springer-Verlag, Berlin, 1985), p. 279.
- ²⁵Z. Z. Wang, M. C. Saint-Lager, P. Monceau, M. Renard, P. Gressier, A. Meerschaut, L. Guemas, and J. Rouxel, *Solid State Commun.* **46**, 325 (1983).
- ²⁶W. Shi, B. J. Wieder, H. L. Meyerheim, Y. Sun, Y. Zhang, Y. Li, L. Shen, Y. Qi, L. Yang, J. Jena *et al.*, *Nat. Phys.* **17**, 381 (2021).
- ²⁷H. Fröhlich, *Proc. R. Soc. London, Ser. A* **223**, 296 (1954).
- ²⁸D. Allender, J. W. Bray, and J. Bardeen, *Phys. Rev. B* **9**, 119 (1974).
- ²⁹D. Schmeltzer and A. Saxena, *Phys. Rev. B* **103**, 235113 (2021).
- ³⁰M.-C. Saint-Lager, P. Monceau, and M. Renard, *Europhys. Lett.* **9**, 585 (1989).
- ³¹R. M. Fleming, R. J. Cava, I. F. Schaefer, E. A. Rietman, and R. G. Dunn, *Phys. Rev. B* **33**, 5450 (1986).
- ³²R. C. McKay and B. Bradlyn, *Phys. Rev. B* **104**, 155120 (2021).
- ³³N. P. Ong, G. Verma, and K. Maki, *Phys. Rev. Lett.* **52**, 663 (1984).
- ³⁴G. Verma and N. P. Ong, *Phys. Rev. B* **30**, 2928 (1984).
- ³⁵A. Zettl, K. Kaiser, and G. Grüner, *Solid State Commun.* **53**, 649 (1985).
- ³⁶Y. You, G. Y. Cho, and T. L. Hughes, *Phys. Rev. B* **94**, 085102 (2016).